Contribution from the J. Heyrovský Institute of Physical Chemistry and Electrochemistry, Dolejškova 3, 182 23 Prague, Czechoslovakia, and Anorganisch Chemisch Laboratorium, J. H. van't Hoff Instituut, Universiteit van Amsterdam, Nieuwe Achtergracht 166, 1018WV Amsterdam, The Netherlands

Nature of the Mn(I)–Dioxolene Bonding as a Function of the Ligand Oxidation State: UV–Vis, IR, and Resonance Raman Spectroelectrochemical Study of $[Mn(CO)_3L_n(Diox)]^z$ (n = 0, 1; z = −2, −1, 0, +1) and $[Mn(CO)_2\{P(OEt)_3\}_m(Diox)]^z$ (m = 1, 2; z = −1, 0, +1) Complexes

František Hartl,[†] Derk J. Stufkens,[‡] and Antonín Vlček, Jr.*[,†]

Received September 19, 1991

The bonding properties of the 3,5-di-*tert*-butyl-1,2-dioxobenzene ligand in the title complexes were experimentally investigated as a function of the dioxolene ligand oxidation state. The electronic absorption spectra are reported for all studied complexes. For pentacoordinated catecholate species and hexacoordinated quinone complexes, resonance Raman spectra were obtained as well. Using these data, the characters of the frontier orbitals of the complex molecules were determined. It follows that π-delocalization exists in the five-coordinated catecholate species where the catecholate ligand behaves as a strong π-donor. The lowest electronic transition is characterized as $\pi \rightarrow \pi^*$ with some LMCT character, the π and π^* orbitals being partly delocalized over the Mn(DBCatecholate)$^-$ chelate ring. This stabilizing π-delocalization is lost in six-coordinated weak adducts with pyridine or $P(OEt)_3$, which possess only the π^*(DBCat) → Mn LMCT transition in the violet region. In the DBSQ complexes, the radical-anionic ligand exerts no special π-bonding properties to the Mn atom. Its spectrum is dominated by a MLCT transition. On the other hand, the quinone ligand is a very strong π-acceptor. The absorption spectrum of $[Mn(CO)_2\{P(OEt)_3\}_2(DBQuinone)]^+$ complex is dominated by an intense absorption band at 582 nm (ϵ = 7400 M^{-1} cm^{-1}). A Raman band at 571 cm^{-1} corresponding to the ν_s(Mn–O) vibration is very strongly enhanced in intensity by resonance with this electronic transition. It points to a very strong π-delocalization within the Mn(DBQ)$^+$ chelate ring, which is probably also the main factor responsible for the unusual chemical stability of this complex. Despite the metal–ligand π-orbital mixing in the catecholate and, especially, quinone complexes, the localized oxidation state picture appears to be appropriate, with the Mn atom possessing a formal oxidation state of I in all studied complexes except $[Mn^0(CO)_3(DBCat)]^{2-}$. The above interpretation of the electronic absorption and resonance Raman spectra is fully supported by IR and EPR data and by the substitution effects on the spectral properties. Strong influence of the change of the number of CO ligands on the electrode potential of the DBSQ/DBQ ligand-localized redox couple is fully in line with the strong delocalization in the quinone complexes.

Introduction

Dioxolenes (i.e. catecholate dianions and their respective oxidation products: semiquinone anion radicals and quinones)[1] are typical noninnocent ligands that retain their redox properties upon coordination to transition metals.[2–4] The availability of three different ligand oxidation states and at least two different oxidation states of the metal leads to intriguing spectral,[5–13] electrochemical,[2–4,6,14–19] and magnetochemical[2,9,10] properties of dioxolene complexes including the possibility of optically induced bistability.[11] The rich redox chemistry is also responsible for the role of these complexes in oxygen transfer reactions[16,20] and various enzymatic processes.[2,5,21]

Recently, we have synthesized and structurally characterized an unusual five-coordinated complex[22] $[Mn(CO)_3(DBCat)]^-$ (**1**) and its substitutional derivative[23] $[Mn(CO)_2\{P(OEt)_3\}(DBCat)]^-$ (**2**). On the basis of their electrochemical behaviour and on the molecular structure of the former complex, manganese was proposed to have the oxidation state (I) and thus a d^6 configuration, while the DBDiox ligand was shown to be present as a catecholate dianion. This conclusion was further supported by the ν(C≡O) vibrational frequencies and the ^1H and ^{13}C NMR spectra. These complexes are rare examples of low-valent carbonyls with electron-rich ligands (π-donors) in their coordination sphere. Their electronic absorption spectra exhibit two bands in the visible region, which were tentatively assigned[22] to DBCat → Mn LMCT transitions. However, the observed spectral pattern and the band intensities strongly resemble those of five-coordinated complexes of d^8 metals[24–27] pointing to a possible ambiguity in the assignment of oxidation states either as Mn^IDBCat or Mn^{-I}DBQ which deserves further investigation.

Both complexes undergo three distinct one-electron redox steps[19,22,23] that correspond to ligand-localized DBCat/DBSQ and DBSQ/DBQ couples and to a Mn(I)/Mn(0) metal-localized couple. We are thus dealing with a structurally homogeneous class of compounds that exist in four different oxidation states. The exceptional stability of all members of this redox series allows to investigate its individual members spectroscopically. Such a study provides a very interesting opportunity to follow the change of

[†] J. Heyrovský Institute of Physical Chemistry and Electrochemistry.
[‡] Universiteit van Amsterdam.

(1) The term "dioxolene" (Diox) is used for ligands derived from 1,2-dioxobenzene irrespective of their oxidation state, i.e. catecholate dianion (Cat), *o*-semiquinone radical-anion (SQ), or *o*-quinone (Q), without specifying the substituents on the benzene ring. The individual oxidation states of 3,5-di-*tert*-butyl-1,2-dioxobenzene (DBDiox) are in this study denoted DBCat, DBSQ, and DBQ.
(2) Pierpont, C. G.; Buchanan, R. M. *Coord. Chem. Rev.* **1981**, *38*, 45.
(3) Auburn, P. R.; Dodsworth, E. S.; Haga, M.; Liu, W.; Nevin, W. A.; Lever, A. B. P. *Inorg. Chem.* **1991**, *30*, 3502.
(4) Downs, H. H.; Buchanan, R. M.; Pierpont, C. G. *Inorg. Chem.* **1979**, *18*, 1736.
(5) Cox, D. D.; Benkovic, S. J.; Bloom, L. M.; Bradley, F. C.; Nelson, M. J.; Que, Jr., L.; Wallick, D. E. *J. Am. Chem. Soc.* **1988**, *110*, 2026.
(6) Haga, M.; Dodsworth, E. S.; Lever, A. B. P. *Inorg. Chem.* **1986**, *25*, 447.
(7) Stufkens, D. J.; Snoeck, T. L.; Lever, A. B. P. *Inorg. Chem.* **1988**, *27*, 953.
(8) Dodsworth, E. S.; Lever, A. B. P. *Chem. Phys. Lett.* **1990**, *172*, 151.
(9) Benelli, C.; Dei, A.; Gatteschi, D.; Pardi, L. *Inorg. Chem.* **1988**, *27*, 2831.
(10) Benelli, C.; Dei, A.; Gatteschi, D.; Pardi, L. *Inorg. Chem.* **1989**, *28*, 1476.
(11) Benelli, C.; Dei, A.; Gatteschi, D.; Pardi, L. *Inorg. Chim. Acta* **1989**, *163*, 99.
(12) Vlčková, B.; Snoeck, T. L.; Stufkens, D. J. *J. Mol. Struct.* **1990**, *218*, 7.
(13) Dei, A.; Pardi, L. *Inorg. Chim. Acta* **1991**, *181*, 3.
(14) Sofen, S. R.; Ware, D. C.; Cooper, S. R.; Raymond, K. N. *Inorg. Chem.* **1979**, *18*, 234.
(15) Bianchini, C.; Masi, D.; Mealli, C.; Meli, A.; Martini, G.; Laschi, F.; Zanello, P. *Inorg. Chem.* **1987**, *26*, 3683.
(16) Bianchini, C.; Frediani, P.; Laschi, F.; Meli, A.; Vizza, F.; Zanello, P. *Inorg. Chem.* **1990**, *29*, 3402.
(17) Bradbury, J. R.; Schultz, F. A. *Inorg. Chem.* **1986**, *25*, 4416.
(18) Gheller, S. F.; Newton, W. E.; de Majid, L. P.; Bradbury, J. R.; Schultz, F. A. *Inorg. Chem.* **1988**, *27*, 359.
(19) Hartl, F.; Vlček, Jr., A. *Inorg. Chem.* **1991**, *30*, 3048.
(20) Barbaro, P.; Bianchini, C.; Mealli, C.; Meli, A. *J. Am. Chem. Soc.* **1991**, *113*, 3181.
(21) Que, L., Jr.; Kolanczyk, R. C.; White, L. S. *J. Am. Chem. Soc.* **1987**, *109*, 5373.
(22) Hartl, F.; Vlček, Jr., A.; deLearie, L. A.; Pierpont, C. G. *Inorg. Chem.* **1990**, *29*, 1073.
(23) Hartl, F. *J. Organomet. Chem.*, in press.

0020-1669/92/1331-1687$03.00/0 © 1992 American Chemical Society

Table I. UV–Vis and IR Spectra of Mn–Carbonyl–Dioxolene Complexes

compound	λ_{max}[a] (ϵ[b])	ν(CO)[c]
$[Mn(CO)_3(DBCat)]^-$ (**1**)[d]	288 (4740)	1994 1891
	436 (6250)	
	546 (8300)	
$[Mn(CO)_3(DBCat)]^-$·py[e]	434 (2200)	1995 1885 1862
$[Mn(CO)_3(DBCat)]^{2-}$[d]	404 (4500)	1890 1769 1749
	536 (2500)	
$[Mn(CO)_2\{P(OEt)_3\}(DBCat)]^-$ (**2**)[f]	290 (4690 sh)	1909 1821
	416 (5500)	
	514 (4200)	
$[Mn(CO)_2\{P(OEt)_3\}_2(DBCat)]^{-}$[f,g]	413 (1700)	1912 1821
	333 (6500 sh)	
$[Mn(CO)_3(PCat)]^-$[d]	450	1990 1887 (sh)
	585	1882
$[Mn(CO)_3(CCat)]^-$[d]	400	2018 1911 (sh)
	505	1906
$[Mn(CO)_3(THF)(DBSQ)]$ (**3**)[d]	310 (9830)	2030 1934
	356 (sh)	1923 (sh)
	524 (2370)	
	708 (1650)	
$[Mn(CO)_2\{P(OEt)_3\}_2(DBSQ)]$ (**4**)[f]	330 (5800)	1946, 1869
	356 (sh)	
	820 (3700)	
$[Mn(CO)_2\{P(OEt)_3\}_2(DBQ)]^+$ (**5**)[f]	392 (2900)	2025, 1965
	582 (7400)	
$[Mn(CO)_2(PPh_3)_2(DBSQ)]$[d,23]	388 (sh)	1927, 1850
	654 (sh)	
	854 (3900)	
$[Mn(CO)_2(PPh_3)_2(DBQ)]^+$[d,23]	388 (7200)	2003, 1943
	610 (6800)	

[a] nm. [b] Extinction coefficient, M^{-1} cm^{-1}. [c] cm^{-1}. [d] In THF. [e] In pyridine. [f] In CH_2Cl_2. [g] −80 °C; actually a weak adduct $[Mn(CO)_2\{P(OEt)_3\}(DBCat)]\cdot P(OEt)_3$; see ref 23.

the character of the DBDiox ligand as a function of its oxidation states using electronic absorption, resonance Raman, and IR spectroscopy. Some fundamental questions concerning both the validity of the oxidation state concept in the dioxolene complexes and the structural factors that determine the particular charge distribution among the metal and the dioxolene ligand may be directly addressed in this way.

Results and Discussion

Catecholate Complexes. The crystal and molecular structure of the Bu_4N^+ salt of $[Mn(CO)_3(DBCat)]^-$ (**1**) points to a small difference in energy between the trigonal bipyramidal and square pyramidal structures, which are both present in the asymmetric region of the unit cell.[22] In order to properly assign the absorption spectra, we have briefly investigated the structures of **1** and of $[Mn(CO)_2\{P(OEt)_3\}(DBCat)]^-$ (**2**) also in solution. The ^{13}C NMR spectrum of the Bu_4N^+ salt of **1** exhibits at 298 K a single CO resonance at 231.2 ppm, $\Delta\nu_{1/2}$ = 28.1 Hz, that splits at about 203 K into a broader peak at 228.4 ppm and a sharp one at 221.3 ppm (δ values obtained at 193 K; $^{13}C\{^1H\}$ NMR spectrum measured in CD_2Cl_2). As the CO ligands are magnetically nonequivalent in the low symmetry of the complex molecule (C_s or no symmetry at all), the carbonyls have to interchange rapidly at room temperature to afford a single ^{13}C NMR peak. The solution IR spectra of **1** and **2** point to the presence of a single species containing a $Mn(CO)_3^+$ unit and a $Mn(CO)_2\{P(OEt)_3\}^+$ unit, respectively. These spectra do not change significantly upon decreasing the temperature from 298 to 193 K. The IR peak corresponding to the $A_1\nu(C\equiv O)$ vibration of **1** shifts from 1998 to 2000 cm^{-1}, and the broad $\nu(C\equiv O)$ band at 1891 cm^{-1} slightly narrows and two maxima show up at 1894 and 1883 cm^{-1}. The

Table II. Standard Electrode Potentials (V vs Fc/Fc^+) of Mn–Carbonyl–Dioxolene Complexes and Free Dioxolene Ligands

compound	solv	potential: Mn^0/Mn^I	Cat/SQ	SQ/Q
$[Mn(CO)_3(DBCat)]^-$ (**1**)	THF	−2.39	−0.70[a]	+0.23[b]
$[Mn(CO)_3(DBCat)]^-$·py	py	−2.39	−0.90[c]	+0.11[d]
$[Mn(CO)_2\{P(OEt)_3\}(DBCat)]^-$ (**2**)	THF[e]	−2.91	−1.25[a,f]	−0.27[g]
	CH_2Cl_2[e]		−1.25[a,f]	−0.37[g]
$[Mn(CO)_4(DBSQ)]$	CH_2Cl_2[h]		−0.80[d]	+0.29
$[Mn(CO)_3(PPh_3)(DBSQ)]$[23]	CH_2Cl_2[i]		−0.92[a]	+0.04
$[Mn(CO)_2(PPh_3)(DBSQ)]$[23]	CH_2Cl_2[i]		−1.23[d]	−0.46
Phenanthrene–Diox	THF		−1.96	−1.20
DBDiox	THF		−1.70	−1.09
Cl_4Diox	THF		−1.32	−0.45

[a] Electrochemically quasireversible, six-coordinated $[Mn(CO)_3(THF)(DBSQ)]$ (**3**) is the oxidized species. [b] Corresponds to the **3**/3^+ couple. [c] Fully reversible; $[Mn(CO)_3(py)(DBSQ)]$ is the oxidized species. [d] Irreversible. [e] In the presence of excess $P(OEt)_3$. [f] Quasireversible, six-coordinated complex **4** is in the oxidized species. [g] **4**/**5** couple. [h] Measured in CO-saturated solution of **1**. [i] Solution of **1** in the presence of excess PPh_3.[23]

solutions of **1** and **2** obviously contain a single, albeit fluxional, structural form as no experimental evidence for the existence of a temperature-dependent equilibrium between different conformations or isomers has been found. In accord with the crystal structure,[22] the molecular structure of **1** in the solution may best be described as a $Mn(CO)_3^+$ trigonal pyramidal fragment of C_{3v} local symmetry that is capped by a chelating DBCat ligand. The spectral and electrochemical properties of **1** and **2** as well as of other investigated complexes are summarized in Tables I and II, respectively. The electronic structure may be easily discussed using the qualitative MO[28] diagram depicted on the right side of Scheme I. One member of the 2e-set of LUMO orbitals of the $Mn(CO)_3^+$ fragment[15,22,28,29] is asymmetric (2e(A)) with respect to the catecholate plane and π-overlaps with the $3b_1$ HOMO[30,31] of the DBCat ligand, producing orbitals (denoted π, π^*) that possess significant π-bonding and π-antibonding character, respectively, with regard to the Mn–O bonds within the $Mn(DBCat)^-$ chelate ring. The other component of the 2e set that is symmetric with respect to the DBCat plane, 2e(s), contributes to the σ-bonding via its interaction[15] with the $7b_2$ combination of the oxygen lone electron pairs.[10,15] Another σ-interaction arises from the overlap between the $2a_1$(S) orbital of the $Mn(CO)_3^+$ fragment and the $9a_1$ combination of the oxygen lone pairs.[10,31] The abovementioned fluxionality can then be viewed as a rotation of the $Mn(CO)_3^+$ unit with respect to the DBCat ligand that preserves the orbital interactions described above. The molecular structures found in the solid state[22] are limiting forms that are stabilized by the crystal lattice.

The solutions of $[Mn(CO)_3(DBCat)]^-$ (**1**) and $[Mn(CO)_2\{P(OEt)_3\}(DBCat)]^-$ (**2**) are intensely wine-red- and red-orange-colored, respectively. The former species exhibits two absorption bands in THF (Figure 1) at 436 nm (ϵ = 6250 M^{-1} cm^{-1}) and 546 nm (ϵ = 8300 M^{-1} cm^{-1}) whose positions are almost solvent-independent: 438, 542 nm in CH_2Cl_2; 435, 549 nm in benzene. The substitution of one CO ligand by $P(OEt)_3$ to give $[Mn(CO)_2\{P(OEt)_3\}(DBCat)]^-$ causes a blue-shift of both bands to 416 nm (ϵ = 5500 M^{-1} cm^{-1}) and 514 nm (ϵ = 4200 M^{-1} cm^{-1}), respectively, in THF (Figure 2).

The characters of the electronic transitions involved were determined by resonance Raman (rR)[32,33] spectroscopy. Although

(24) Dawson, J. W.; McLennan, T. J.; Robinson, W.; Merle, A.; Dartiguenave, M.; Dartiguenave, Y.; Gray, H. B. *J. Am. Chem. Soc.* **1974**, *96*, 4428.
(25) Dawson, J. W.; Venanzi, L. M.; Preer, J. R.; Hix, J. E., Jr.; Gray, H. B. *J. Am. Chem. Soc.* **1971**, *93*, 778.
(26) Dawson, J. W.; Gray, H. B.; Hix, J. E., Jr.; Preer, J. R.; Venanzi, L. M. *J. Am. Chem. Soc.* **1972**, *94*, 2979.
(27) Preer, J. R.; Gray, H. B. *J. Am. Chem. Soc.* **1970**, *92*, 7306.
(28) Albright, T. A.; Burdett, J. K.; Whangbo, M. H. *Orbital Interactions in Chemistry*; Wiley-Interscience: New York, 1985.
(29) Elian, M.; Hoffmann, R. *Inorg. Chem.* **1975**, *14*, 1975.
(30) The $3b_1$ orbital[10,15,31] is strongly π-antibonding with respect to the C–O bonds, weakly C_3–C_4 and C_5–C_6 π-antibonding, and weakly C_1–C_2 π-bonding. It is a frontier orbital of dioxolene ligands, being the LUMO of the quinone, the SOMO of the semiquinone anion radical, and the HOMO of the catecholate dianion. The symmetry label refers to the C_{2v} point group of an idealized ligand. Its energy decreases going from DBCat to DBSQ to DBQ.
(31) Gordon, D. J.; Fenske, R. F. *Inorg. Chem.* **1982**, *21*, 2907.

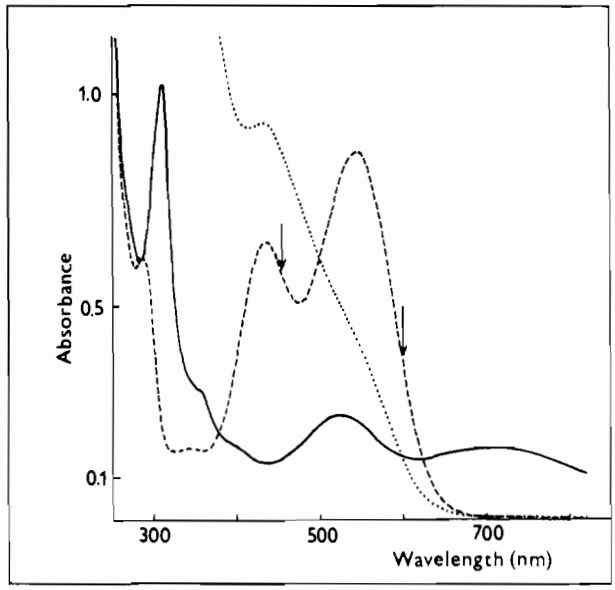

Figure 1. Electronic absorption spectra of 1.04×10^{-4} M $Bu_4N[Mn(CO)_3(DBCat)]$ $[Bu_4N(1)]$ (--) and $[Mn(CO)_3(THF)(DBSQ)]$ (**3**) (—) in THF and of 8.2×10^{-4} M $Bu_4N[Mn(CO)_3(DBCat)]$ $[Bu_4N(1)]$ in pyridine (···) at ambient temperature. The arrows indicate the laser wavelengths used to measure the rR spectra.

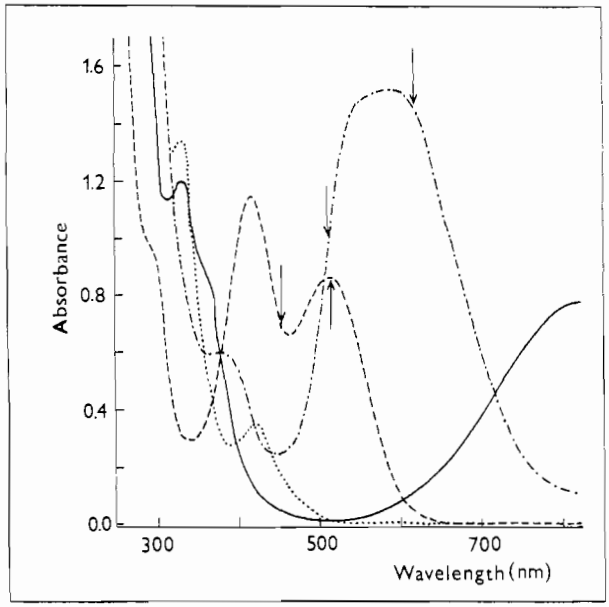

Figure 2. Electronic absorption spectra of $Bu_4N[Mn(CO)_2\{P(OEt)_3\}(DBCat)]$ $[Bu_4N(2)]$ at ambient temperature in THF (--) and at 193 K in CH_2Cl_2 (···), and $[Mn(CO)_2\{P(OEt)_3\}_2(DBSQ)]$, (**4**) (—), and $[Mn(CO)_2\{P(OEt)_3\}_2(DBQ)]BF_4$ [(**5**)BF_4] (-·-), both at ambient temperature in THF. The concentration of all complexes was 2.1×10^{-4} M. Excess $P(OEt)_3$ was present in all solutions. The arrows indicate the laser wavelengths used to measure the rR spectra.

only the spectra measured at one excitation wavelength within each absorption band are reported below, the resonant enhancement of the Raman peaks was proven by a significant decrease of their intensity when the excitation wavelength approached the low-energy end of the absorption bands. The assignment of the Raman peaks was quite straightforward as the positions of the DBCat-vibrations are very similar to those found and previously assigned for $[Fe^{III}(Schiff\text{-}base)(catecholate)]$ complexes[5] and the peaks corresponding to the $\nu(C{\equiv}O)$ vibrations were observed in the IR spectra at identical wavenumbers.

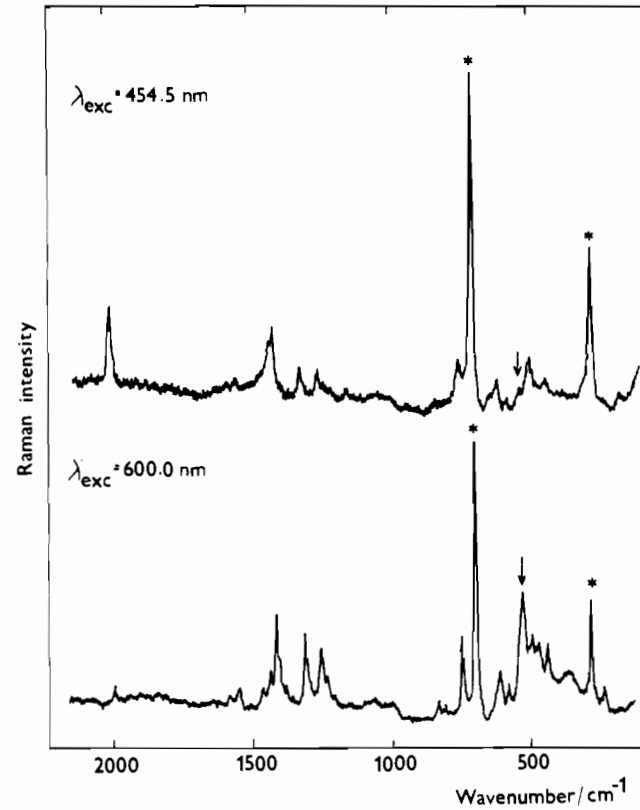

Figure 3. Resonance Raman spectra of $Bu_4N[Mn(CO)_3(DBCat)]$ $[Bu_4N(1)]$ excited at 454.5 and at 600 nm. Measured in CH_2Cl_2 at ambient temperature in 1-cm quartz cell. An asterisk denotes peaks due to CH_2Cl_2. The arrow indicates the band belonging to the ν_s(Mn–O) chelate-ring vibration.

To elucidate the nature of the low-energy band, the rR spectra of Bu_4N^+ salts of **1** and **2** were measured using the 600 and 514.5 nm laser lines, respectively (Figures 3 and 4). Apart from the 530 cm^{-1} band of complex **1** (vide infra), the most significantly enhanced vibrations are those corresponding to the DBCat ligand at 1410, 1316, and 1254 cm^{-1} for **1** and at 1413, 1318, and 1254 cm^{-1} for **2**. By analogy with the data in ref 5, the feature at 1254 cm^{-1} is assigned to the C–O stretch of the DBCat ligand, the band at 1316–1318 cm^{-1} to a skeletal mode of the DBCat ring and the band at 1410–1413 cm^{-1}, to a C–C stretching vibration. Several weak bands due to C–C and DBCat-ring vibrations[5] occur at 1551, 1463, 1434, 611, and 580 cm^{-1} for **1** and at 1546, 1462, 1434, and 607 cm^{-1} for **2**. The Raman band corresponding to the Mn–O–C–C–O chelate-ring vibration (further to be denoted as ν_s(Mn–O)) occurs, in the case of **1**, at 530 cm^{-1} its intensity being enhanced to the same extent as the intensity of the strongest peaks due to the DBCat vibrations. The Raman peak belonging to the corresponding mode of **2** at 526 cm^{-1} is also enhanced, albeit to a smaller extent. This chelate-ring vibration is actually a symmetric stretch of both Mn–O bonds partially coupled with the C_1–C_2 vibration[5,7,34] of the DBCat ring. Other weakly enhanced skeletal vibrations are observed at 240 cm^{-1} for both **1** and **2** and at 440 cm^{-1} for **1**. (The "bump" in the low-frequency region apparent in the spectra is due to the quartz cell. The complete assignment of weak bands in this region was not attempted.) The enhancement of the $\nu(C{\equiv}O)$ Raman band is very weak.

On the basis of these rR spectra, the low-energy absorption band of both complexes **1** and **2** may straightforwardly be assigned to a $\pi \rightarrow \pi^*$ transition of the $Mn(DBCat)^-$ chelate ring (see Scheme I). The depopulation of an orbital that is π-bonding with respect to the Mn–O bonds (π, Scheme I) with a concomitant population of a corresponding π-antibonding orbital (π^*, Scheme I) causes

(32) Clark, R. J. H.; Dines, T. J. *Angew. Chem., Int. Ed. Engl.* **1986**, *25*, 131.
(33) Stufkens, D. J. *J. Mol. Struct.* **1982**, *79*, 1982.
(34) Nakamoto, K. *Infrared and Raman Spectra of Inorganic and Coordination Compounds*, 4th ed.; Wiley-Interscience: New York, 1986; pp 244–245.

Scheme I. Qualitative MO Diagram for $[Mn(CO)_3L_n(DBDiox)]^a$ (n = 0, 1; a = −2, −1, 0, +1) Complexes[a]

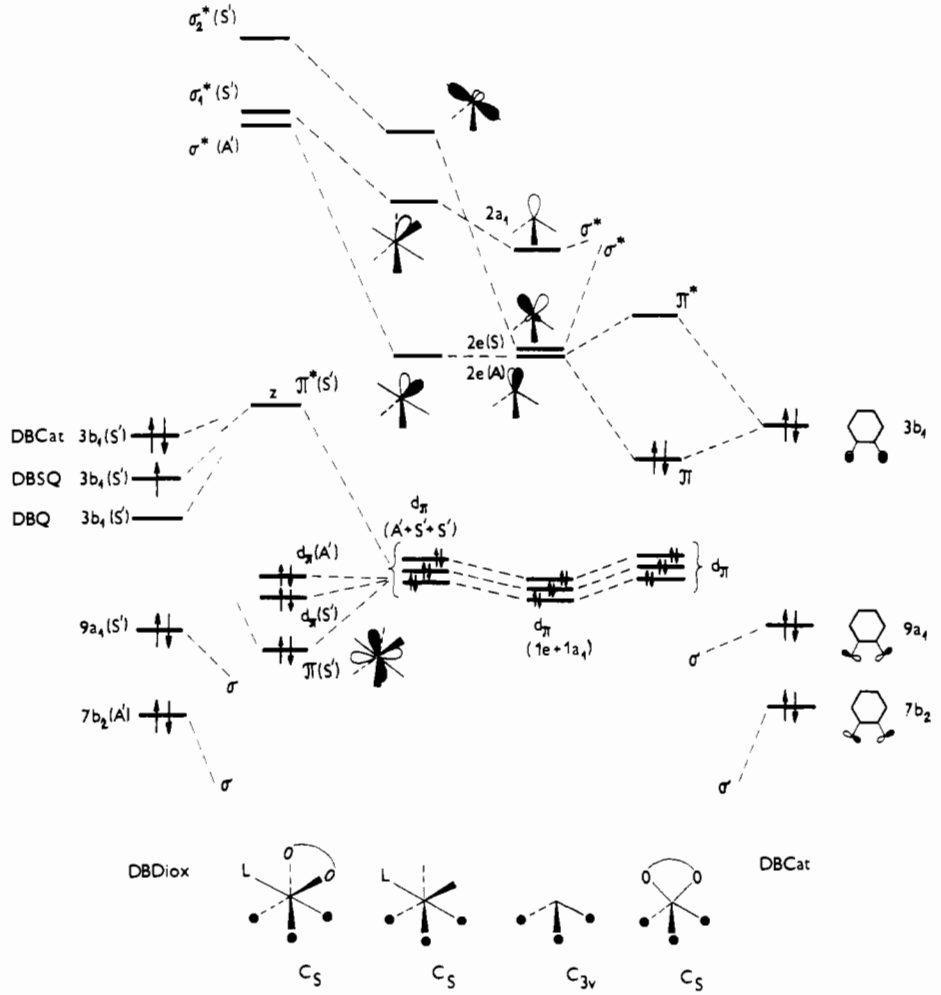

[a] The MO levels of the pentacoordinated DBCat complexes (n = 0; a = −1, −2) are on the right-hand side of the scheme. They are derived by combining the orbitals of the $Mn(CO)_3^+$ fragment[28,29] with those of the DBCat ligand.[10,15,30,31] The summary labels (A, S) refer to the DBCat molecular plane. The MO levels of the hexacoordinated species (n = 1; a = −1, 0, +1) are on the left-hand side of the scheme. The orbitals of the $Mn(CO)_3L^+$ fragment were derived from those of $Mn(CO)_3^+$ without changing the molecular orientation. The $3b_1$ frontier orbital of DBDiox ligand decreases in energy going from DBCat to DBSQ to DBQ. The energy of the $\pi^*(S')$ orbital of the Mn(DBDiox) chelate ring changes accordingly as discussed in the text. The number of electrons in the $\pi^*(S')$ orbital is the same as in the $3b_1$ one, i.e. z = 2, 1, and 0 for DBCat, DBSQ, and DBQ, respectively. The summary labels (A', S') refer to the plane of symmetry that bisects the DBCat molecular plane.

significant changes in the Mn–DBCat bonding, and hence, the Raman band corresponding to the ν_s(Mn–O) vibration is enhanced. This observation points to an orbital mixing (i.e. π-delocalization) within the $Mn(DBCat)^-$ chelate ring that is in full accord with the arguments used[22] to explain the stability of the unusual five-coordination in **1**. However, the Raman bands corresponding to DBCat ligand vibrations are enhanced as well in the rR spectra showing that the mixing between the DBCat-$3b_1$ and Mn-2e(A) orbitals is not complete, presumably because of their energy difference. The participation of the $3b_1$ orbital in the π-orbital prevails, and therefore, its depopulation during the electronic excitation affects the bonds within the DBCat ligand. The $\pi \rightarrow \pi^*$ transition thus has partial LMCT character. Apparently, the π-delocalization is less extensive in the case of the substituted complex **2** since the ν(Mn–O) vibration is much less enhanced with respect to the intraligand DBCat modes than in the case of **1**. The $\pi \rightarrow \pi^*$ transition in **2** has thus more LMCT character. The lower extinction coefficient of the corresponding absorption band of **2** is in accord with this interpretation. The smaller extent of the 2e(A)–$3b_1$ interaction in **2** is caused by the increase in energy of the 2e(A) orbital due to its involvement in the σ-bonding with a stronger base $P(OEt)_3$ and also due to the higher electron density on the Mn atom caused by the higher σ-basicity and lower π-acidity of $P(OEt)_3$ compared with CO. This energy increase of the 2e(A) orbital energy leads in turn to an increase in energy of the π^*-LUMO orbital, which was experimentally indicated by the negative shift of the Mn^I/Mn^0 reduction potential of **2** with respect to that of **1** by 450 mV,[23] i.e. 3630 cm^{-1} (Table II). However, the decrease of the strength of the $3b_1$–2e(A) interaction in **2** also increases the π-orbital energy, and consequently, the low-energy absorption band shifts to higher energy in going from **1** to **2** by only 1140 cm^{-1}.

Excitation with the 454.5-nm laser line into the high-energy electronic absorption band of both complexes leads to a very significant intensity enhancement of the Raman band belonging to the symmetric $\nu(C{\equiv}O)$ vibration at 1998 cm^{-1} for **1** and at 1909 cm^{-1} for **2**. Obviously, a member of the d_π set of orbitals that is involved in the Mn → CO π-back-bonding (see Scheme I) participates in the electronic transition.[35] Raman peaks belonging to the DBCat-ligand vibrations at 1410, 1316, and 1254 cm^{-1} and at 1413, 1318, and 1254 cm^{-1} for **1** and **2**, respectively,

(35) A resonant enhancement of the $\nu(C{\equiv}O)$ vibration in the Raman spectra measured by the excitation into the MLCT band of $M(CO)_4(\alpha,\alpha'$-dimine) type complexes (M = Cr, Mo, W) has been explained by a through-space interaction between the π^*-orbitals of the CO and α-diimine ligands, the latter one being populated by electronic excitation (Balk, R. W.; Snoeck, T. L.; Stufkens, D. J.; Oskam, A. *Inorg. Chem.* **1980**, *19*, 3015. Balk, R. W.; Stufkens, D. J.; Oskam, A. *Inorg. Chim. Acta* **1979**, *34*, 267). However, this mechanism cannot operate in the present case as, due to the pentacoordination, the CO and DBCat ligands are too far away from each other[22] in a pentacoordinated complex, making the overlap of their π^*-orbitals impossible.

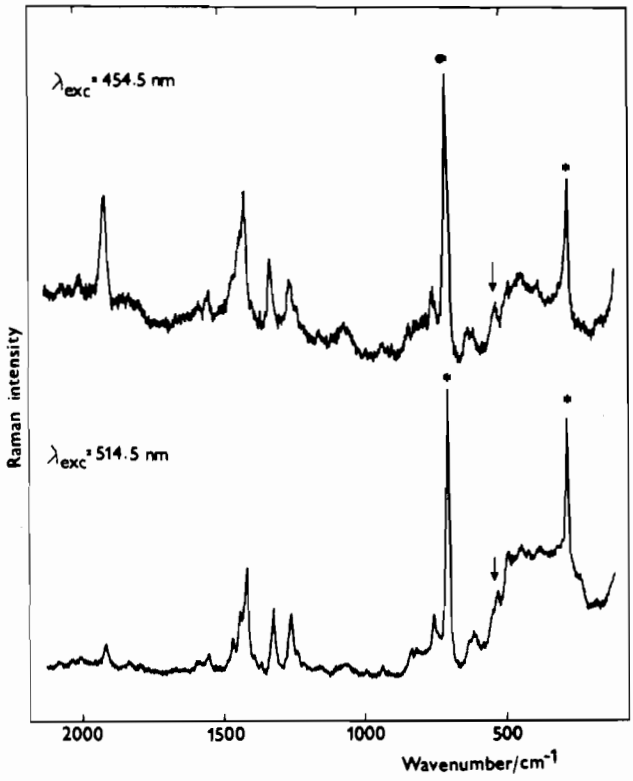

Figure 4. Resonance Raman spectra of $Bu_4N[Mn(CO)_2\{P(OEt)_3\}(DBCat)]$ [Bu_4N(**2**)] excited at 454.5 and at 514.5 nm. Measured in CH_2Cl_2 at ambient temperature in 1-cm quartz cell. An asterisk denotes peaks due to CH_2Cl_2. The arrow indicates the band belonging to the ν_s(Mn–O) chelate-ring vibration.

are also enhanced in intensity (Figures 3 and 4). The same vibrations were enhanced, albeit more strongly, also upon excitation into the low-energy absorption band, and also the relative intensity pattern is the same (vide supra). The ν_s(Mn–O) chelate ring vibrations at 530 cm^{-1} (**1**) and 526 cm^{-1} (**2**) are present in the spectra, although with low intensity. (A larger intensity enhancement of ν_s(Mn–O) in **2** is probably due to the overlap between both electronic absorption bands at 454.5 nm.) Except for the ν(C≡O) Raman band and smaller enhancement of the ν_s(Mn–O) peak, the rR spectra observed upon excitation into the high-energy band qualitatively parallel those measured using the excitation into the low-energy one (vide supra). This observation shows that the other orbital involved in the high-energy transition is the same as that participating in the low-energy one, i.e. the π^*-orbital. As this orbital is antibonding with respect to the Mn–O bonds, the ν_s(Mn–O) vibration is enhanced. The admixture of the $3b_1$ orbital then leads to the enhancement of the DBCat vibrations.

The high-energy transition is thus assigned as $d_\pi \rightarrow \pi^*$, the d_π orbital being a member of the $1a_1 + 1e$ set of the orbitals of the $Mn(CO)_3^+$ fragment that are π-bonding with respect to the Mn–CO bonds.[28,29] As the π^*-orbital is for large part a 2e(A) d orbital (vide supra), the $d_\pi \rightarrow \pi^*$ transition may be viewed as being partially a d → d one. This is not in contrast to its high intensity because of the participation of the $3b_1$ ligand orbital, admixture of the 4p character,[28] and a low molecular symmetry. The $d_\pi \rightarrow \pi^*$ transition is shifted by 1103 cm^{-1} to higher energy in going from **1** to **2**. As in the case of the $\pi \rightarrow \pi^*$ transition, this effect is much less than could be expected on the basis of the electrochemical data that point to a destabilization of the π^*-orbital by 3630 cm^{-1}; vide supra. This can be explained by the concomitant increase in the d_π-orbital energy due to increased electron density on the Mn atom. However, the latter effect is partially compensated by an increase in the Mn → CO back-bonding within the $Mn(CO)_2\{P(OEt)_3\}^+$ structural unit as evidenced by a large decrease, by 89 cm^{-1}, in the ν(C≡O) frequencies in going from **1** to **2**; see Table I.

The above assignment of the spectral bands to $d_\pi \rightarrow \pi^*$ and $\pi \rightarrow \pi^*$ transitions is also in accord with the influence of the changing electron-donating properties of the Cat ligand. The absorption maxima occur at 450 and 585 nm for $[Mn(CO)_3$(phenanthrene–catecholate)$]^-$ and at 400 and 505 nm for $[Mn(CO)_3$(tetrachlorocatecholate)$]^-$. Both bands thus shift to higher energy going from PCat to DBCat and to CCat, in parallel with the increasing potential of the Cat/SQ redox couple of the free ligand (Table II), i.e. with decreasing energy of the $3b_1$ HOMO and thus also decreasing π-donating strength. As a result, the π-orbital of the complex is stabilized and its $3b_1$ character increases. Again, the $\pi \rightarrow \pi^*$ spectral shifts are smaller than those expected from the electrochemical data due to the compensating effect of the π-delocalization within the $Mn(Cat)^-$ ring. (If the π-orbital was purely $3b_1$, a blue-shift by 3065 cm^{-1} could be expected on going from the DBCat to the CCat complex.) The decrease in the electron density on the Mn atom (evidenced by the increase of the $A_1\nu$(C≡O) frequency, Table I) stabilizes the occupied d_π orbitals, thus also increasing the energy of the $d_\pi \rightarrow \pi^*$ transition, which acquires more dd character on going to the CCat complex. (The comparison of extinction coefficients was precluded by the fact that the PCat complex is only a component of an equilibrium and by an instability of the CCat species.[23])

Interestingly, the spectral patterns found for both **1** and **2** (Figures 1 and 2) closely resemble those observed by Venanzi, Gray, et al. for d^8-pentacoordinated complexes and assigned to d → d transitions.[24-27] However, the metal and ligand oxidation states of **1** (as derived from its molecular structure) undoubtedly correspond to Mn^IDBCat^-, i.e. to a d^6 configuration, as the bond lengths within the $Mn(DBDiox)^-$ moiety of **1** fit very well into the range typical for the DBCat ligand.[3,22] Moreover, the electrochemical reduction of both **1** and **2** produces Mn(0) complexes, whereas their oxidation is ligand-localized, leading to Mn^I(DBSQ) complexes.[19,22,23] This also shows that the redox oxidation states[36] can be assigned as d^6 Mn^IDBCat. Nevertheless, an intriguing possibility exists that the spectroscopic oxidation state[37] differs from the structural and redox ones and that **1** and **2** can alternatively be formulated, at least from the spectroscopic point of view, as $Mn^{-I}(DBQ)^-$. To solve this possible ambiguity, the spectra of **1** and **2** were compared with those of the d^8 systems in more detail. A typical feature of the d → d transitions of the d^8 systems is an intense broad band that exhibits two maxima which correspond to the same electronic transition split by a Jahn–Teller effect and show a profound temperature dependence of both their intensities and band shapes.[25,26] Neither of these features were found in our case. Moreover, the highest separation of the absorption band maxima found for the d^8 species is 3750 cm^{-1}, i.e. significantly less than the separation between the high- and low-energy peaks in **1** and **2**: 4621 and 4583 cm^{-1}. Most importantly, the band maxima of **1** and **2** correspond to different electronic transitions as was proven by the rR spectra. Consequently, the resemblance between the spectral patterns of **1** and **2** and those of five-coordinated complexes of d^8 metals is only phenomenological and the spectral assignment of the oxidation states in both **1** and **2** agrees with that based on redox[19,23] and structural[22] arguments, i.e. $Mn^I(DBCat)^-$.

In conclusion, the electronic absorption spectra show that there is a π-delocalization in the ground states of both **1** and **2** which amounts to a significant transfer of electron density from the DBCat ligand to the Mn atom. This is clearly reflected in the ν(C≡O) frequencies of **1** (1994, 1891 cm^{-1}) and **2** (1909, 1821 cm^{-1}) which are much lower compared with those of manganese(I) tricarbonyl complexes with ligands lacking π-properties.[38] However, the electronic absorption and rR spectra also show that the ligand $3b_1$ character still prevails in the HOMO of the complex molecule. This means that the delocalization is not extensive enough to alter the formal oxidation states.

(36) Vlček, A. A. *Rev. Chim. Miner.* **1968**, *6*, 299.
(37) Jörgensen, C. K. *Structure and Bonding*; Springer-Verlag Berlin: 1966, Vol. 1, p 234.
(38) van der Graaf, T.; Stufkens, D. J.; Vichová, J.; Vlček, A., Jr. *J. Organomet. Chem.* **1991**, *401*, 305.

Catecholate complexes usually exhibit a $3b_1 \rightarrow 4b_1$ intraligand transition in the UV region. In both **1** and **2**, this absorption is shifted to higher energy compared with the DBCat complexes[10,11,13,39,40] of Co(III), Rh(III), Ni(II), and Cu(II). The UV absorption band of **1** occurs at 288 nm (4740 M^{-1} cm^{-1}) and at 290 nm (sh, ϵ = 4690 M^{-1} cm^{-1}) for **2**. The blue-shift is explained by the involvement, and thus stabilization, of the $3b_1$ orbital by the π-bonding with Mn. It is thus more appropriate to describe this transition as $\pi \rightarrow 4b_1$ in the case of **1** and **2**.

Complexes **1** and **2** are both photochemically stable in pure CH_2Cl_2 as well as in the presence of excess PPh_3 or $P(OEt)_3$. This photostability is in full accord with the delocalized character of the $\pi\pi^*$ lowest excited state. The stability of the complex molecule against dissociation is not greatly diminished by the electronic excitation as the Mn–CO bonds are not affected and the weakening of the π-bonding within the $Mn(DBCat)^-$ chelate ring does not overcome rather strong σ-bonding that is unchanged in this excited state. The lifetime of the $\pi\pi^*$ excited state can also be expected to be rather short because of the activation of the low-frequency ν(Mn–O) vibration that could provide an effective deactivation pathway.[41]

Complex **1** associates[23] reversibly with pyridine and, at low temperatures, also with phosphines, increasing thus its coordination number to 6. Although this coordination is rather weak, it has a profound effect on the visible absorption spectra. In pure pyridine, the absorption spectrum of **1** (Figure 1) exhibits a maximum at 434 nm (ϵ = 2200 M^{-1} cm^{-1}), which occurs as a shoulder on a broad absorption band. Complex **2** associates reversibly with $P(OEt)_3$ at low temperature. The absorption spectrum of **2** was measured at 193 K in CH_2Cl_2 in the presence of excess $P(OEt)_3$ (Figure 2). A single maximum developed at 413 nm (ϵ = 1700 M^{-1} cm^{-1}) on the low-energy side of a much stronger UV absorption (shoulder at 333 nm, ϵ = 6500 M^{-1} cm^{-1}). These spectral changes which are caused by the change of coordination number from 5 to 6 can be explained using the left side of Scheme I. (Note that the symbols S′ and A′ denote the orbital symmetry with respect to the plane *bisecting* the Cat-molecular plane whereas S and A are related to the Cat *molecular* plane.) The 2e(A) orbital responsible for the π-bonding with the DBCat ligand in the five-coordinated complexes becomes involved in the Mn–L σ-bonding in the six-coordinated species (σ_2^*(S′)), and it is therefore strongly raised in energy. In the six-coordinated geometry, the $3b_1$(S′) HOMO of the DBCat ligand can thus effectively π-interact only with the occupied d_π(S′) orbital that is perpendicular to the DBCat molecular plane. This interaction results in π(S′) and π^*(S′) orbitals. The $3b_1$–d_π energy gap is rather large and the π^*(S′) has thus predominantly $3b_1$ ligand character. The π-delocalization within the Mn(DBCat) chelate ring no longer exists, and the $\pi \rightarrow \pi^*$ transition disappears. As both π(S′) and π^*(S′) orbitals are occupied, the $d_\pi \rightarrow \pi^*$ transition disappears as well. The observed absorption band of the hexacoordinate adducts of both **1** and **2** is assigned to a π^*(S′) $\rightarrow$ σ^*(A′) LMCT transition that is symmetry-allowed but overlap-forbidden. As a result, its intensity is low compared with the transitions observed in the parent five-coordinated complexes. The stronger absorption in the near-UV region probably belongs to a π^*(S′) $\rightarrow$ σ^*(S′) transition.

The reduction of **1** produces[19,22,42] a Mn(0) complex, $[Mn(CO)_3(DBCat)]^{2-}$. Its absorption spectrum is very similar to that of **1**, both bands being slightly shifted to higher energy and significantly reduced in intensity: 404 (ϵ = 4500 M^{-1} cm^{-1}) and 536 nm (ϵ = 2500 M^{-1} cm^{-1}). As in **1**, these bands are assigned to $d_\pi \rightarrow \pi^*$ and $\pi \rightarrow \pi^*$ transitions, the π^*-orbital being the SOMO of the complex molecule. The effect of the reduction on the electronic spectrum of **1** is qualitatively analogous to the effect of the substitution of a CO ligand by a stronger donor like $P(OEt)_3$ because of the increased electron density on Mn.

Semiquinone complexes $[Mn(CO)_3L(DBSQ)]$ and $[Mn(CO)_2L_2(DBSQ)]$ are formed by electrochemical or chemical (usually using Cp_2Fe^+) oxidation[19,22] of the $[Mn(CO)_3(DBCat)]^-$ complex in the presence of an excess of the ligand L. They can also be conveniently generated by a photolysis of $Mn_2(CO)_{10}$ with DBQ and a wide variety of Lewis bases L.[38,43,44] All of these complexes are six-coordinated.

The electronic absorption spectrum of $[Mn(CO)_3THF(DBSQ)]$ (**3**) exhibits two bands in the visible region at 524 nm (ϵ = 2370 M^{-1} cm^{-1}) and 708 nm (ϵ = 1650 M^{-1} cm^{-1}) (Figure 1). The visible absorption in the substituted complex $[Mn(CO)_2\{P(OEt)_3\}_2(DBSQ)]$ (**4**) is rather broad and strongly red-shifted: 820 nm (ϵ = 3700 M^{-1} cm^{-1}), extending into the near-IR region (Figure 2). On the basis of Scheme I (left side), the 524 nm band of **3** is assigned to a π(S′) $\rightarrow$ π^*(S′) transition, the π^*(S′) being the SOMO of the complex molecule. The red shift of the absorption maximum by 6890 cm^{-1} going from **3** to **4** is in line with the above assignment as a significant destabilization of the d_π orbitals upon substitution of one CO by $P(OEt)_3$ is expected due to an increase of electron density on the Mn atom which is clearly manifested by a significant decrease of ν(C≡O) frequencies going from **3** to **4**, see Table I. Further red shift of the band maximum accompanied by a decrease in ν(C≡O) frequencies was observed (Table I) going from **4** to an analogous $[Mn(CO)_2(PPh_3)_2(DBSQ)]$ complex as PPh_3 is a stronger base and a weaker π-acceptor than $P(OEt)_3$. Although the $3b_1$ orbital is lower in energy compared with the DBCat ligand, it is still the main component of the π^*(S′) orbital whereas the π(S′) orbital is mainly a d_π one. The spectral transition may clearly be regarded as a MLCT one.

In this case, it was not possible to measure the rR spectra as both DBSQ complexes rapidly photodecomposed under laser excitation. The photoproducts were not identified. However, the rR spectra we have obtained[45] for the analogous Re complexes $[Re(CO)_3(PPh_3)(DBSQ)]$, $[Re(CO)_2(PPh_3)_2(DBSQ)]$, and $[Re(CO)_4(DBSQ)]$ fully support the assignment of the main visible absorption band to a MLCT transition.

The weaker band at 708 nm is, in analogy with other DBSQ complexes, assigned to an essentially intraligand $9a_1$(S′) $\rightarrow$ π^*(S′)($3b_1$) transition which is very typical for DBSQ complexes of various metals.[8-13,40] In complex **4**, this transition is probably hidden under the broad absorption in the red region. The alternative assignment as a d_π(S′) $\rightarrow$ π^*(S′) transition cannot completely be excluded, although this would require the splitting of the original d_π set by as much as 4960 cm^{-1}, which seems improbable.

A strong, narrow UV absorption band was observed at 310 nm (ϵ = 9830 M^{-1} cm^{-1}) with a shoulder at 356 nm for **3** and at 330 nm (ϵ = 5800 M^{-1} cm^{-1}) with a shoulder at 356 nm for **4** (Figures 1 and 2). Such an intense UV absorption is very typical for all DBSQ metal complexes[9-11,13,40] as well as for an uncoordinated DBSQ.[46] It is usually assigned to an intraligand transition not shown in Scheme I. The π^*(S′) $\rightarrow$ dσ^*(A′ or S′) LMCT transition that was observed in the case of $[Mn(CO)_3L(DBCat)]^-$ adducts (vide supra) is most probably hidden under the UV-absorption; perhaps it manifests itself as a shoulder at 356 nm. Its blue-shift with respect to the hexacoordinated adducts of the DBCat complexes is expected as the $3b_1$ orbital, and thus also the π^*(S′) orbital, is stabilized by the change of the ligand oxidation state to DBSQ.

The assignment of the visible absorption band to a MLCT transition is in full accord with our previous conclusions on the lack of any significant π-bonding (i.e. d_π–$3b_1$ orbital mixing) between the DBSQ radical-anionic ligand and the Mn atom, which were based on the EPR and IR spectra of the $[Mn(CO)_3L$-

(39) Wicklund, P. A.; Brown, D. G. *Inorg. Chem.* **1976**, *15*, 396.
(40) Benelli, C.; Dei, A.; Gatteschi, D.; Pardi, L. *Inorg. Chem.* **1990**, *29*, 3409.
(41) Servaas, P. C.; van Dijk, H. K.; Snoeck, T. L.; Stufkens, D. J.; Oskam, A. *Inorg. Chem.* **1985**, *24*, 4494.
(42) Krejčík, M.; Daněk, M.; Hartl, F. *J. Electroanal. Chem. Interfacial Electrochem.* **1991**, *317*, 179.
(43) Vlček, A. *J. Organomet. Chem.* **1986**, *306*, 63.
(44) Abakumov, G. A.; Cherkasov, V. K.; Shalnova, K. G.; Teplova, I. A.; Razuvaev, G. A. *J. Organomet. Chem.* **1982**, *236*, 333.
(45) Hartl, F.; Stufkens, D. J.; Vlček, A., Jr. *Inorg. Chim. Acta*, in press.
(46) Stallings, M. D.; Morrison, M. M.; Sawyer, D. T. *Inorg. Chem.* **1981**, *20*, 2655.

(DBSQ)] complexes.[38] Moreover, the present study shows that further substitution of CO by phosphites or phosphines increases the π-bonding within the Mn(DBSQ) chelate ring. This is evident from the larger Mn-splitting constants in the EPR spectra of **4** compared with those measured for tricarbonyls: a_{Mn} = 16.0 G for **4** whereas 3.7 G was found[38] for **3**. The closer proximity of the d_π and $3b_1$ orbitals caused by the destabilization of the d_π level in the substituted species is responsible for this effect (vide supra). The increase of the ν(C≡O) frequencies by 40–50 cm^{-1} caused by the oxidation of the DBCat ligand in **1** to DBSQ in **3** (Table I) is quite large, taking into account that the Mn oxidation state was not changed and a Lewis base was coordinated. Similarly, complex **4** exhibits ν(C≡O) frequencies that are higher by some 40 cm^{-1} than those of the DBCat complex **2**. This points to a large decrease of the electron density on Mn by the oxidation of the DBCat ligand, which causes a loss of its π-donating properties.

Quinone Complexes. The $[Mn(CO)_2\{P(OEt)_3\}_2(DBQ)]^+$ (**5**) complex was generated spectroelectrochemically by employing the electrochemical oxidation of $[Mn(CO)_2\{P(OEt)_3\}(DBCat)]^-$ in CH_2Cl_2 in the presence of an excess of free $P(OEt)_3$ at potentials more positive than –0.38 V vs the Fc/Fc^+ couple. Alternatively, it can be prepared[23] from the $[Mn(CO)_2\{P(OEt)_3\}_2(DBSQ)]$ complex using Cp_2FeBF_4 as an oxidizing agent. The $[Mn(CO)_3(THF)(DBQ)]^+$ and $[Mn(CO)_4(DBQ)]^+$ complexes that were observed by cyclic voltammetry[19] are less amenable for spectroscopic studies since they have more positive redox potentials and a lower chemical stability.

The electronic absorption spectrum of **5** (Figure 2) exhibits a band at 392 nm (ϵ = 2900 M^{-1} cm^{-1}), tentatively assigned to an intraligand transition, and a band with an apparent maximum at 582 nm (ϵ = 7400 M^{-1} cm^{-1}) that obviously encompasses several, most probably three, spectral transitions which, according to scheme I, can be assigned to $d_\pi \rightarrow \pi^*(S')$ transitions originating from different members of the original set of d_π orbitals. Complex **5** slowly disproportionated, producing the DBSQ complex **4**, which was detected by IR spectroscopy together with some other, unidentified, products. Although this disproportionation is slightly accelerated by irradiation with 514.5- and 620-nm laser light, the rR spectra of **5** could still be measured (Figure 5) using a Raman instrument with a diode-array detection and keeping the potential of the working electrode above –0.38 V during the whole experiment. In this way the photolytically or thermally formed **4** was immediately reoxidized to **5**. There is a good evidence that the observed Raman peaks indeed belong to the DBQ complex **5**: (i) the disproportionation product **4** does not absorb at 514.5 nm and its Raman bands therefore can not be resonantly enhanced, (ii) no new Raman bands were found in the spectra upon going from 514.5- to 620-nm excitation, excluding thus the possibility of interference with the spectrum of the photolytic product **4**, and (iii) oxidation of complex **4** to **5** in an IR–spectroelectrochemical cell in CD_3CN solution caused the appearance of the IR peaks (1366, 642, 590, 455 cm^{-1}) of **5**, which closely corresponded to those observed in the rR spectra.

At both excitation wavelengths, the rR spectrum is dominated by a strongly enhanced peak at 571 cm^{-1}. All peaks due to the internal vibrations of the DBQ ligand are only weakly enhanced. They occur at 1410, 1362, 1310, 1154, 742, 638 cm^{-1} and even less enhanced peaks were found at 1240, 1209, 931, and 905 cm^{-1}. This rR spectral pattern closely resembles that of the $[Rubpy_2(BQ)]^{2+}$ complex, BQ being the unsubstituted 1,2-benzoquinone.[7] By this analogy, the main peak at 571 cm^{-1} is attributed to the ν_s(Mn–O) vibration of the $Mn(DBQ)^+$ chelate ring. Other vibrations in this frequency region (589, 525, 453 cm^{-1}) most probably also belong to the skeletal vibrations of the chelate ring.[7] Corresponding Raman peaks are significantly enhanced in intensity but to a lesser extent than the peak due to the ν_s(Mn–O) vibration at 571 cm^{-1}. Interestingly, no enhancement of the ν(C≡O) vibration was observed. The rR spectrum points to a strongly delocalized $\pi(S') \rightarrow \pi^*(S')$ transition that dominates the absorption band at both excitation wavelengths. Hence, the $\pi(S')$ and $\pi^*(S')$ orbitals of the $Mn(DBQ)^+$ chelate ring (see Scheme I, left) should be regarded as strongly intermixed $d_\pi(S') + 3b_1(S')$ and $d_\pi(S') - 3b_1(S')$ combinations, respectively. A transition between such orbitals does not affect the population of the $d_\pi(S')$ and $3b_1(S')$ orbitals, and, hence significant rR effects are expected neither for the DBQ ligand vibration nor for the ν(C≡O) modes. On the other hand, the excitation causes the population of an orbital that is π-antibonding with respect to the Mn–O bonds, and as a result, the ν(Mn–O) vibration will strongly be affected. Transitions from the other two d_π orbitals which do not directly interact with the $3b_1$ orbital are present within the same band envelope, influencing its shape. Their presence may be partly responsible for the small enhancement of the DBQ ligand vibrations. A substitution of a $P(OEt)_3$ ligand in **5** by more Lewis basic PPh_3 may be expected to further destabilize the d_π orbitals, leading to a red-shift of the $\pi(S') \rightarrow \pi^*(S')$ transition as was, indeed, observed (Table I).

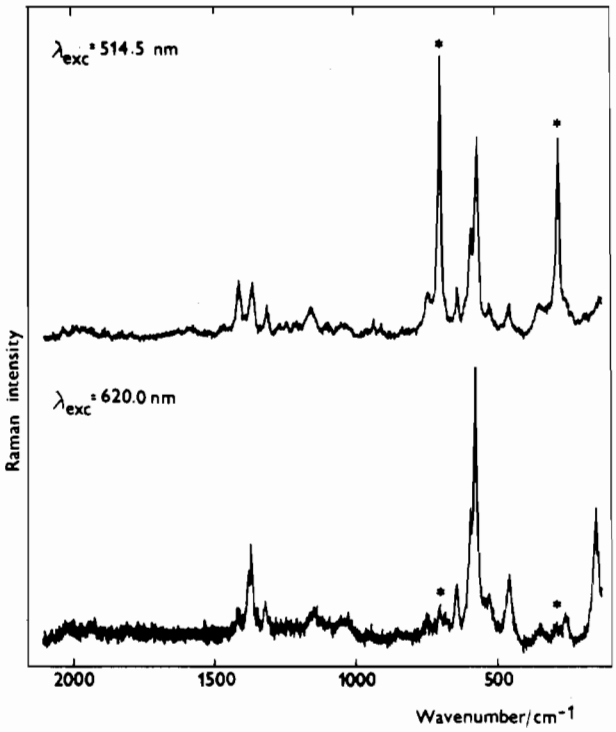

Figure 5. Resonance Raman spectra of $[Mn(CO)_2\{P(OEt)_3\}_2(DBQ)]^+$, (**5**) excited at 514.5 and 620 nm, measured in CH_2Cl_2 at ambient temperature. Complex **5** was generated by a spectroelectrochemical oxidation of **2** on a Pt-mesh working electrode in CH_2Cl_2 containing 10^{-1} M Bu_4NPF_6 with a small excess of $P(OEt)_3$ using an IR-OTTLE cell equipped with NaCl windows.

The $\pi(S') \rightarrow \pi^*(S')$ transition in the quinone complex **5** occurs at an energy approximately 4360 cm^{-1} higher than observed in the semiquinone species **4**. An analogous blue-shift was found[6] going from $[Rubpy_2SQ]^+$ to $[Rubpy_2Q]^{2+}$ complexes. It was attributed[6] to a higher distortion of the excited state in the DBQ complex, which requires an excitation into a Franck–Condon state that is highly vibrationally excited; i.e., the excitation energy involves a large contribution from the inner reorganization energy.[6] We prefer, however, the more simple explanation that the mixing between the $3b_1$ and $d_\pi(S')$ orbitals is much stronger in the case of the DBQ than the DBSQ complex because of the lower $3b_1$ orbital energy of DBQ compared with DBSQ. Such an interaction pushes the π- and π^*-orbitals apart increasing thus the energy gap and the excitation energy. Both explanations are fully in line with the rR data, and they may complementarily apply to both the Ru and Mn complexes.

Unexpectedly, the substitution of one CO by $P(OEt)_3$ in the $Mn(CO)_3^+$ unit has a strong influence on the redox potential of the ligand-localized DBQ/DBSQ couple. Whereas the $[Mn(CO)_3L(DBSQ)]/[Mn(CO)_3L(DBQ)]^+$ (L = CO, THF, PPh_3) couples occur at +0.29, +0.23, and +0.04 V, respectively, the **4**/**5** couple was found at –0.36 V in CH_2Cl_2 and at –0.27 V in THF. Analogously, the potential of the $[Mn(CO)_2(PPh_3)_2(DBSQ)]/$

$[Mn(CO)_2(PPh_3)_2(DBQ)]^+$ couple is −0.46 V. This high negative shift observed in going from tri- to dicarbonyls is another, albeit indirect, piece of evidence for the delocalized π-bonding within the $Mn(DBQ)^+$ moiety. Obviously, the $\pi^*(S')$-orbital energy in the dicarbonyls is substantially higher than in the tricarbonyl ones due to the $3b_1$–$d_\pi(S')$ mixing which is stronger in the substituted complexes **5** and $[Mn(CO)_2(PPh_3)_2(DBQ)]^+$ because of the destabilization of the d_π levels by the strongly σ-donating $P(OEt)_3$ and PPh_3 (vide supra). On the other hand, the DBSQ/DBQ potential is only slightly sensitive to the nature of the sixth ligand (L = THF, CO, PPh_3) in the $[Mn(CO)_3L(DBDiox)]$ species (Table II). This is in full accord with the bonding pattern proposed in Scheme I.

An interesting question arises whether the assignment of the oxidation states $Mn(I)(DBQ)^+$ is still valid or whether the complex molecule should instead be viewed as a $Mn^{II}(DBSQ)$ species. Usually,[2,3,6,14-19] the oxidation of the DBSQ ligand precedes that of the metal. In our previous electrochemical study,[19] the stability of the $Mn(CO)_3^+$ unit was used as an argument in favor of the assignment of the most positive oxidation step as a DBSQ/DBQ instead of a Mn(I)/Mn(II) one. The $\nu(C\equiv O)$ frequencies of **5** occur at 2025 and 1964 cm^{-1} in CH_2Cl_2, i.e. 79 and 95 cm^{-1}, respectively, higher than those of the DBSQ complex **4**. This is a large shift; nevertheless, the absolute magnitude of the $\nu(C\equiv O)$ frequencies is comparable with those of other manganese(I) tricarbonyl complexes.[34,38] The intense visible absorption band is rather typical for DBQ complexes. A similar band was found in $[Rubpy_2(Q)]^{2+}$ and in $[Ru(NH_3)_4(BQ)]^{2+}$ complexes.[6,7,47] The available data thus agree with the formulation of **5** as a $Mn^I(DBQ)$ complex, the DBQ ligand possessing very strong π-acceptor properties.

To our knowledge, only very few quinone complexes of transition metals are known.[3] The exceptional stability of complex **5** and of[6,7] $[Rubpy_2Q]^{2+}$ may be due to a strongly delocalized π-bonding within the $M(DBQ)^+$ chelate ring that is common for both types of complexes as indicated by an analogous electronic absorption and resonance Raman spectra. Most other quinone complexes were detected only electrochemically or spectroelectrochemically. Those of more electropositive metals like Co(III),[11,15] Ni(II),[9] and Mo(VI)[17] are very labile even on the time scale of cyclic voltammetry and usually undergo a loss of the DBQ ligand. This is presumably due to the fact that, in complexes of metals in higher oxidation states, the d_π orbitals are either empty or too low-lying to interact effectively with the $3b_1$ LUMO of the DBQ ligand.

Conclusions

1. The nature of the DBDiox ligand varies, depending on its oxidation state, from a strong π-donor DBCat through almost π-nonbonding DBSQ to a very strong π-acceptor DBQ. The DBCat ligand, when coordinated to a d^6 metal, can exert its π-donor properties only in a five-coordinated complex. These profound changes in the DBDiox π-bonding ability give rise to a very significant dependence of the $\nu(C\equiv O)$ vibration frequencies on the oxidation state of the DBDiox ligand. Vice versa, the electronic effects caused by CO substitution in the $Mn(CO)_3^+$ fragment are, through a delocalized π-bonding, transmitted to the DBDiox ligand. This is manifested by a dependence of the potentials of the redox steps localized on the DBDiox ligand on the composition of the rest of the coordination sphere.

2. Spectroscopically, this varying nature of the DBDiox ligand manifests itself by changing the character of the lowest electronic transition. The five-coordinated DBCat complexes are characterized by a partly delocalized LMCT transition. The presence of rather pure MLCT transitions is typical for DBSQ species, while the DBQ complexes exhibit very delocalized ML transitions.

3. The changing nature of the DBDiox ligand also determines the chemical behavior of the complex. The partly delocalized Mn←(DBCat) π-bonding is the main factor that stabilizes the five-coordinated DBCat complexes **1** and **2** against an uptake of Lewis bases. This type of interaction is lost upon the oxidation of the DBCat ligand, and the corresponding DBSQ and DBQ complexes are invariably six-coordinated.[19,23] The strong Mn → DBQ π-bonding in the DBQ complexes **5** and $[Mn(CO)_2(PPh_3)_2(DBQ)]^+$ (and probably also in their tricarbonyl analogues and related Re species) is responsible for their stability against the substitution of the DBQ ligand. The delocalized bonding within the Mn(DBDiox) chelate ring also appears to be responsible for the photostability of the DBCat and DBQ complexes.

Experimental Section

Materials. 3,5-Di-*tert*-butyl-1,2-benzoquinone, DBQ (Aldrich), was recrystallized from *n*-heptane. Phenanthrenequinone, 3,4,5,6-tetrachloro-1,2-benzoquinone and PPh_3 were used as obtained from Aldrich. Bu_4NPF_6 (Fluka) was dried in vacuo at 350 K for 10 h. $P(OEt)_3$ (Fluka) was distilled under reduced pressure and deoxygenated before use. $[Cp_2Fe]BF_4$ was synthesized by a published method.[48] All solutions for spectroscopic studies were freeze–pump–thaw degassed and handled under high vacuum. Solvents (all of spectroscopic grade) were freshly distilled under argon atmosphere and degassed on a vacuum line. THF (Fluka) was distilled from a sodium–benzophenone mixture and CH_2Cl_2 (Fluka) from P_2O_5. CD_3CN (Merck) was stored under argon over Linde type 4A molecular sieves. Pyridine (Merck) was dried by refluxing with solid KOH, followed by fractional distillation.

$Bu_4N[Mn(CO)_3(DBCat)]\cdot{}^1/_6C_6H_6$ was prepared and characterized according to ref 22. $Bu_4N[Mn(CO)_2\{P(OEt)_3\}(DBCat)]$ was generated[23] in a CH_2Cl_2 solution by the substitution reaction of the parent tricarbonyl complex **1** with a small excess of $P(OEt)_3$. The formation and purity of the substituted product **2** was checked by FTIR spectroscopy.[23] The reduced species $[Mn(CO)_3(DBCat)]^{2-}$ was electrochemically generated within the IR spectroelectrochemical OTTLE (optically transparent thin-layer electrochemical) cell as described in ref 42. $[Mn(CO)_3(THF)(DBSQ)]$ was formed in situ in the THF solution either by oxidation[19] of $Bu_4N[Mn(CO)_3(DBCat)]$ with $[Cp_2Fe]BF_4$ in THF or by spectroelectrochemical oxidation[42] on a Pt-mesh electrode in an infrared spectroelectrochemical (OTTLE) cell. Its IR and EPR spectra agree with those published previously.[38,43,44] $[Mn(CO)_2\{P(OEt)_3\}_2(DBSQ)]$ was generated in situ[23] in THF solution either from $[Mn(CO)_3(THF)(DBSQ)]$ by its substitution reaction with $P(OEt)_3$ or in CH_2Cl_2 by the reaction of equivalent amounts of $Bu_4N[Mn(CO)_2\{P(OEt)_3\}(DBCat)]$ and $[Mn(CO)_2\{P(OEt)_3\}_2(DBQ)]BF_4$. It was characterized by EPR and FTIR spectroscopy.[23] $[Mn(CO)_2\{P(OEt)_3\}_2(DBQ)]BF_4$ was generated[23] in CH_2Cl_2 by spectroelectrochemical oxidation on a Pt-mesh electrode or in THF, by a chemical oxidation of $Bu_4N[Mn(CO)_2\{P(OEt)_3\}(DBCat)]$ with $[Cp_2Fe]BF_4$. $[Mn(CO)_2(PPh_3)_2(DBSQ)]$ was generated in situ by a substitution reaction of **3** with excess PPh_3 in THF at 40 °C. Its spectroelectrochemical or chemical (using $[Cp_2Fe]BF_4$) oxidation afforded $[Mn(CO)_2(PPh_3)_2(DBQ)]^+$. Both $PPN[Mn(CO)_3(PCat)]$ and $PPN[Mn(CO)_3(CCat)]$ were generated in solution and characterized in situ by IR and UV–vis spectroscopy.

PPN[Mn(CO)$_3$(PCat)]. A 8.5-mg (0.04-mmol) sample of phenanthrenequinone (PQ) in THF (6 mL) was added dropwise under the Ar atmosphere to stirred THF (6 mL) solution containing 30 mg (0.04 mmol) of $PPN[Mn(CO)_5]$. The color of the solution changed immediately to blue owing to the formation of $PPN[Mn(CO)_3)(PCat)]$, which gave IR $\nu(C\equiv O)$ bands at 1990, 1887 sh, and 1882 cm^{-1} and UV–vis absorption bands with maxima at 450 and 585 nm. The resulting blue solution was EPR silent. Intense bands at 1891 and 1861 cm^{-1} due to $Mn(CO)_5^-$ are still present in the IR spectrum, pointing to an equilibrium between the reactants and $[Mn(CO)_3(PCat)]^-$. Addition of a small excess of PQ to the reaction mixture shifted the equilibrium toward the product formation.

PPN[Mn(CO)$_3$(CCat)]. The reaction between $PPN[Mn(CO)_5]$ and 3,4,5,6-tetrachloro-1,2-benzoquinone, CQ, in CH_2Cl_2 proceeded more slowly compared with the PQ case. The light yellow color of the CH_2Cl_2 solution containing 10 mg (0.014 mmol) of $PPN[Mn(CO)_5]$ gradually changed to red-orange upon dropwise addition of 1 molar equiv (3.4 mg, 0.014 mmol) of CQ in CH_2Cl_2. The $PPN[Mn(CO)_3(CCat)]$ product is characterized by IR $\nu(C\equiv O)$ bands at 2018, 1911 (sh), and 1906 cm^{-1} and by absorption bands at 400 and 505 nm in the visible region. The reaction mixture exhibits other, less intense $\nu(C\equiv O)$ bands at 2046, 2011, 1977, 1894, and 1861 cm^{-1}, assigned to traces of unreacted $Mn(CO)_5^-$ and to $Mn_2(CO)_{10}$, the latter being formed by an outer-sphere electron transfer that takes place between $Mn(CO)_5^-$ and CQ in parallel with dominant $2e^-$ oxidative substitution, which produces $[Mn(CO)_3(CCat)]^-$.

(47) Pell, S. D.; Salmonsen, R. B.; Abelleira, A.; Clarke, M. J. *Inorg. Chem.* **1984**, *23*, 385.

(48) Hendrickson, D. N.; Sohn, Y. S.; Gray, H. B. *Inorg. Chem.* **1971**, *10*, 1559.

Instrumentation. Hewlett-Packard 8452A diode-array and Carl-Zeiss-Jena M40 spectrometers were used to measure the electronic absorption spectra. The IR spectra were recorded on Philips PU9800 FTIR and Nicolet 7199B FTIR spectrometers at resolutions of 4 and 1 cm^{-1}, respectively. EPR spectra were measured using a Varian E4 X-band spectrometer. The temperature-dependent $^{13}C\{^1H\}$ NMR spectra were recorded on a Bruker AM 400 instrument. The resonance Raman spectra were measured with a Dilor XY spectrometer with excitation by the lines of a SP 2016 Ar^+ laser or by a CR-590 dye laser employing Coumarine 6 or Rhodamine 6G dyes pumped by the Ar^+ laser. The solutions of both DBCat complexes **1** and **2** were placed in 1-cm quartz cells. Resonance Raman spectra of all other compounds were measured by employing an IR-OTTLE cell[42] equipped with a Pt-minigrid working electrode (6 × 5 mm rectangle; 32 wires/cm) and NaCl windows. The laser beam was directed at the surface of the working electrode, and the back-scattered light was detected. The same infrared OTTLE cell was also employed to measure IR (with KBr windows) and UV–vis spectra (with CaF_2 windows) of the spectroelectrochemically generated DBSQ and DBQ complexes. The controlled-potential electrolyses within the OTTLE cell were carried out using a Model PA4 polarographic analyser (Laboratorní Přístroje, Prague) or a PAR Model 173 potentiostat equipped with Instruments) x-y recorders, respectively. All potentials are referenced to that of the Fc/Fc^+ couple.[49] The low-temperature IR measurements were performed using an Oxford Instruments DN 1704/54 liquid-nitrogen cryostat. The low-temperature UV–vis spectra were obtained with a Leybold Heraeus ROK 10-300 refrigerator-controlled helium cryostat. The sample solutions in standard 1cm cuvettes were sealed under high vacuum and placed in a homemade Cu sample holder.

Acknowledgment. Theo L. Snoeck (Universiteit van Amsterdam) is thanked for his technical assistance with the measurement of the resonance Raman spectra. We greatly appreciate the financial support from the Universiteit van Amsterdam (A.V.) and from the "John van Geuns" fund (F.H.).

(49) Gagné, R. R.; Koval, C. A.; Lisensky, C. G. *Inorg. Chem.* **1980**, *19*, 2854.

Contribution from the Department of Chemistry, University of New Mexico, Albuquerque, New Mexico 87131, and Institut für Anorganische Chemie, Universität München, 8000-München 2, FRG

Synthesis and Chemistry of Diborylphosphanes

Danan Dou,[†] Gary L. Wood,[†] Eileen N. Duesler,[†] Robert T. Paine,*[,†] and H. Nöth*[,‡]

Received September 24, 1991

Syntheses for $(i\text{-}Pr_2N)_2BP(SiMe_3)_2$ and $(i\text{-}Pr_2N)_2BPH_2$ from $(i\text{-}Pr_2N)_2BCl$ and $LiP(SiMe_3)_2$ or $LiPH_2$ and for $\{[Li\cdot DME][(i\text{-}Pr_2N)_2BP(H)]\}_2$ from $(i\text{-}Pr_2N)_2BPH_2$ and BuLi are described. The species $\{[Li\cdot DME][(i\text{-}Pr_2N)_2BP(H)]\}_2$ is a useful synthon for diborylphosphines, and preparations of $[(i\text{-}Pr_2N)_2B]_2PH$, $Ph_2NB[P(H)B(i\text{-}Pr_2N)_2]_2$, and $[(i\text{-}Pr_2N)_2B][(R_2N)(Cl)B]PH$ (R_2N = i-Pr_2N, tmp, $[Me_3Si]_2N$) are presented. Metal carbonyl coordination chemistry and selected substitution chemistry of these reagents are also described. The molecular structures of $\{[Li\cdot DME][(i\text{-}Pr_2N)_2BP(H)]\}_2$ (**3**), $[(i\text{-}Pr_2N)_2B][tmpB(Cl)]PH$ (**7**), $[(i\text{-}Pr_2N)_2B][tmpB(Cl)]PH\cdot Cr(CO)_5$ (**13**), and $[(i\text{-}Pr_2N)_2B]_2PH\cdot Cr(CO)_5$ (**12**) have been determined by single-crystal X-ray diffraction analyses: **3** ($C_{16}H_{39}BLiN_2O_2P$) crystallizes in the monoclinic space group $P2_1/n$ with a = 9.458 (2) Å, b = 22.054 (3) Å, c = 11.574 (2) Å, β = 111.86 (1)°, and Z = 4; **7** ($C_{21}H_{47}B_2N_3PCl$) crystallizes in the monoclinic space group $P2_1/n$ with a = 16.661 (3) Å, b = 9.218 (2) Å, c = 18.068 (4) Å, β = 103.88 (3) Å, and Z = 4; **13** ($C_{26}H_{47}B_2N_3O_5PClCr$) crystallizes in the triclinic space group $P\bar{1}$ with a = 10.395 (2) Å, b = 10.923 (2) Å, c = 15.800 (3) Å, α = 103.51 (2)°, β = 83.92 (2)°, γ = 104.45 (2)°, and Z = 2; **12** ($C_{29}H_{57}B_2N_4O_5PCr$) crystallizes in the monoclinic space group $P2_1/n$ with a = 10.534 (2) Å, b = 19.991 (4) Å, c = 18.005 (4) Å, β = 95.16 (3)°, and Z = 4.

Introduction

Elimination reactions between appropriate phosphane and borane reagents produce a variety of monomeric phosphinoboranes, R_2PBX_2, small-ring phosphinoboranes $(R_2PBX_2)_n$ (n = 2, 3), and polymeric compounds.[1-21] Recent reevaluations of this chemistry have indicated that there are additional synthetic objectives that may be achieved with this chemistry.[22-51] In particular, it has been revealed that novel, multiply bonded species and clusters can be obtained by careful design of precursors. In this regard, our groups have found that phosphinoboranes with diethylpropyl, trimethylsilyl, or hydrogen substituents on phosphorus are particularly useful precursors.[43,46-51] In this report, the utilization of $\{[Li\cdot DME][(i\text{-}Pr_2N)_2BP(H)]\}_2$ to prepare diborylphosphines $[(i\text{-}Pr_2N)_2B]_2PH$, $Ph_2NB[P(H)B(i\text{-}Pr_2N)_2]_2$, and $[(i\text{-}Pr_2N)_2B][(R_2N)(Cl)B]PH$ is described along with selected chemistry of these reagents.

Experimental Section

General Information. Standard inert-atmosphere techniques were used for the manipulation of all reagents and reaction products. Infrared spectra were recorded on a Nicolet 6000 FT-IR spectrometer from solution cells or KBr pellets. Mass spectra were obtained from a Finnegan mass spectrometer by using a GC inlet system or heated solids probe. NMR spectra were recorded on Bruker WP 250 and JEOL GSX-400 spectrometers. All NMR samples were sealed in 5-mm tubes with a deuterated lock solvent, and the spectra were referenced with Me_4Si (^{13}C, ^1H), $BF_3\cdot Et_2O$ (^{11}B), LiBr (^7Li), and 85% H_3PO_4 (^{31}P). Elemental

[†] University of New Mexico.
[‡] Universität München.

(1) Reviews of phosphinoborane chemistry appear in the following: *Developments in Inorganic Polymers*; Lappert, M. F., Leigh, G. L., Eds.; Elsevier Publ. Co.: New York, 1962. Muetterties, E. L. *The Chemistry of Boron and its Compounds*; J. Wiley: New York, 1967.
(2) Sowerby, D. B. *The Chemistry of Inorganic Homo- and Heterocycles*; Haiduc, I., Sowerby, D. B., Eds.; Academic Press: New York, 1987; Vol. I, Chapter 3.
(3) Parshall, G. W.; Lindsay, R. V. *J. Am. Chem. Soc.* **1959**, *81*, 6273.
(4) Leffler, A. J.; Teach, E. G. *J. Am. Chem. Soc.* **1960**, *82*, 2710.
(5) Burg, A. B.; Wagner, R. I. *J. Am. Chem. Soc.* **1978**, *75*, 3872.
(6) Goodrow, M. H.; Wagner, R. I.; Stewart, R. D. *Inorg. Chem.* **1964**, *3*, 1212.
(7) Goodrow, M. H.; Wagner, R. I. *Inorg. Chem.* **1976**, *15*, 2830; **1976**, *15*, 2836; **1976**, *17*, 350.
(8) Sens, M. A.; Odom, J. D.; Goodrow, M. H. *Inorg. Chem.* **1976**, *15*, 2825.
(9) Wiberg, E.; Nöth, H. *Z. Naturforsch.* **1957**, *12b*, 125.
(10) Nöth, H.; Schrägle, W. *Z. Naturforsch.* **1961**, *16b*, 473.
(11) Nöth, H.; Schrägle, W. *Chem. Ber.* **1965**, *98*, 352.
(12) Nöth, H.; Schrägle, W. *Chem. Ber.* **1964**, *97*, 2218.
(13) Nöth, H.; Schrägle, W. *Chem. Ber.* **1964**, *97*, 2374.
(14) Nöth, H.; Schrägle, W. *Angew. Chem.* **1962**, *1*, 457.
(15) Becker, W.; Nöth, H. *Chem. Ber.* **1972**, *105*, 1962.
(16) Coates, G. E.; Livingstone, J. C. *J. Chem. Soc.* **1961**, 5053.
(17) Coates, G. E.; Livingstone, J. C. *J. Chem. Soc.* **1961**, 1000.
(18) Tevebaugh, A. D. *Inorg. Chem.* **1964**, *3*, 302.
(19) Mayer, E.; Laubengayer, A. W. *Monatsch. Chem.* **1970**, *101*, 1138.
(20) Fritz, G.; Sattler, E. *Z. Anorg. Allg. Chem.* **1975**, *413*, 193.
(21) Fritz, G.; Hölderich, W. *Z. Anorg. Allg. Chem.* **1977**, *431*, 61.
(22) Arif, A. M.; Boggs, J. E.; Cowley, A. H.; Lee, J. G.; Pakulskin, M.; Power, J. M. *J. Am. Chem. Soc.* **1986**, *108*, 6083.
(23) Arif, A. M.; Cowley, A. H.; Pakulskin, M.; Power, J. M. *J. Chem. Soc., Chem. Commun.* **1986**, 889.
(24) Escudie, J.; Couret, C.; Lazraq, M.; Garrigues, B. *Synth. React. Inorg. Met.-Org. Chem.* **1987**, 379.

0020-1669/92/1331-1695$03.00/0 © 1992 American Chemical Society